SAND2019-13764C

Method to Interface Grid-Forming Inverters into Power Hardware in the Loop

Javier Hernandez-Alvidrez, Nicholas S. Gurule, Adam Summers
Matthew J. Reno, Jack D. Flicker, Abraham Ellis
Sandia National Laboratories
Albuquerque, NM, USA

***Abstract*—Recently, power converters with grid-forming capabilities have attracted interest from researchers and utilities as a keystone converter control scheme enabling modern microgrid architectures. Therefore, proper and thorough testing of these grid-forming inverters (GFMIs) is crucial to understand their dynamic limitations before they are deployed. The use of closed-loop real-time Power Hardware-in-the-Loop (PHIL) simulations will facilitate the testing of GFMIs using a digital twin of the power system under various contingency scenarios within a controlled environment. This paper addresses a method to interface commercially available GFMIs with a PHIL testbed. Experimental results show that the proposed method is stable and accurate under standalone operation with abrupt (step) load-changing dynamics, followed by the corresponding steady state behavior. Such results were validated against the dynamics of the GFMI connected to a load bank.**

***Index Terms*—Grid-forming inverters, microgrids, power converters, power hardware in the loop, simulation models.**

I. Introduction

Lately, interactions of aging transmission infrastructure with adverse natural conditions; such as high winds, wildfires, heat waves, and hurricanes; have drastically exposed the vulnerabilities of large power grids under overload conditions. As blackouts have become more severe in terms of duration and frequency of occurrence, grid-resiliency will play a significant role in the modernization of transmission and distribution systems around the world [1]. As the state-of-practice is transitioning from reactive to resilient [2], microgrids will play a crucial role in incorporating renewable and energy storage Distributed Energy Resources (DERs), as well as in mitigating grid contingencies such as low impedance faults and unplanned islanding conditions [3]. Modern microgrids rely on power electronic interfaces not only to regulate the energy flow between DERs while monitoring and maintaining stability, but also to provide ancillary services during grid contingencies [4]. In the case of grid-following inverters (GFLIs), these services are in the form of smart functions such as: volt-var, frequency-watt, and fixed power factor [5], [6]. The main drawback of GFLIs is that they require a voltage reference to synchronize their internal phase locked loop (PLL) and operate properly [7]. This functionality makes them suitable for grid-tied operation, but not under islanded conditions since they do not provide grid-forming capabilities. For this reason, grid-forming inverters (GFMIs) are a feasible solution for islanded scenarios where power needs to be supplied to costumers while regulating voltage and frequency locally without the inertia from a bulk-grid interconnection [8]. GFMI control schemes are still under development, but currently there are three main categories of control schemes being considered:

- Droop-control: where a linear relationship is established between the real and reactive powers delivered by the GFMI and regulated frequency and voltage [9],[10].
- Virtual synchronous machines: where the equations governing the dynamics of the GFMI emulate the behavior of synchronous machines and the intrinsic inertia of these machines is modeled in a virtual fashion [11].
- Virtual oscillator control (VOC): where the control of the GFMI is based upon the dynamics of non-linear oscillators and their corresponding limit cycles [12],[13].

Recently, academics, researchers at different national laboratories, and practicing design and utility engineers gathered together to discuss and review the tendencies and advances in the area of microgrids under low inertia constraints [14]. The three aforementioned GFMIs control schemes were thoroughly reviewed by highlighting their advantages and disadvantages, not only at single-unit functional level, but also at systemic level while interacting with protection and monitoring equipment such as protective relays and smart sensing devices. While the state-of-practice for interconnecting and operating DERs has evolved over the last decade, there are well-defined industry standards, guides, and best practices that dictate and regulate their behavior [15]–[17]. If GFMIs are to abide by such standards, thorough and rigorous tests must be performed to validate their functionality under steady-state and contingency scenarios. For these types of tests, the use of real-time simulators are very attractive since they provide the computational resources to simulate a variety of complex systems, while also allowing the interconnection and control of four-quadrant power amplifiers, which can be interfaced with power electronic devices. This configuration is referred to as Power Hardware in the Loop (PHIL), and allows the testing of commercially available equipment, such as GFLIs and GFMIs,

under different power-transferring conditions within a controlled environment [18].

PHIL simulation setups for GFLIs are well documented in terms of analytical procedures to improve stability and accuracy. Furthermore, these methods have been validated with experimental results [18]–[21]. However, the interfacing of GFMIs into PHIL simulation setups is lightly documented [22].

A common PHIL setup is shown in Fig. *1*. Notice that the Point of Common Coupling (PCC) between the Device Under Test (DUT) and the power amplifier is a direct connection between the terminals of both devices. If the DUT is a GFLI, and the power amplifier is properly rated to fit the GFLI's power capabilities, then the PLL of the GFLI uses the voltage provided by the power amplifier as a reference to synchronize and deliver the commanded real and reactive powers. Conversely, if the DUT is a GFMI, then a direct connection with the power amplifier at PCC can lead to instability, and eventually to catastrophic damage of one or both devices. This is caused because both devices inherently try to regulate the voltage and frequency at the PCC, which leads to instability due to the lack of voltage angle synchronization between the two devices [9]. Therefore, a proper interfacing method for GFMIs must be addressed.

This paper presents a novel, simple, and accurate method to interface commercially available GFMIs into PHIL setups. As described in further sections, the interaction between the power amplifier and the GFMI is modified in such a way that a direct connection between them is avoided whilst maintaining simulation accuracy and system stability.

II. Analytical Background

If real and reactive power transfer between two voltage sources is required, a passive element such a reactor needs to be connected between the two sources as depicted in Fig. 2. Also note that the parasitic resistances of the windings of the inductor and contactor (R_{tot}) are included. Once the contactor is closed, the equations that govern the power flow between the two devices are as follows:

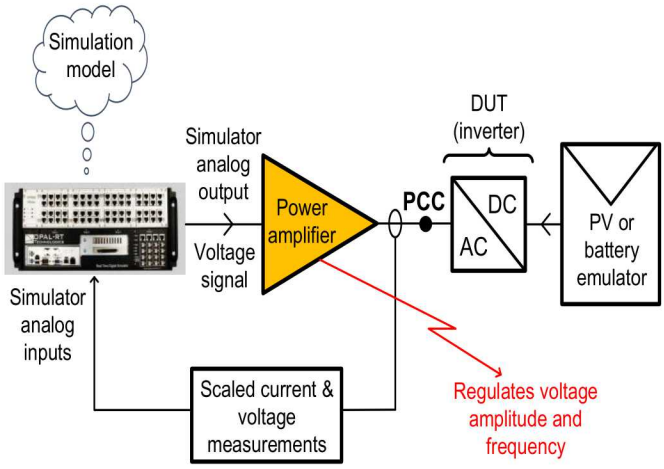

Fig. 1 Common PHIL setup [22],[23].

$$P = \frac{R_{tot}(V_i^2 - V_i V_g \cos\delta) + X_L V_i V_g \sin\delta}{R_{tot}^2 + X_L^2} \quad (1)$$

$$Q = \frac{X_L(V_i^2 - V_i V_g \cos\delta) + R_{tot} V_i V_g \sin\delta}{R_{tot}^2 + X_L^2} \quad (2)$$

Where X_L is the reactance of the inductor and δ is the angle difference between the two voltage sources. If R_{tot} is neglected in (1) and (2), the simplified equations are:

$$P = \frac{V_i V_g \sin\delta}{X_L} \quad (3)$$

$$Q = \frac{V_i^2 - V_i V_g \cos\delta}{X_L} \quad (4)$$

Since the proposed method relies on the equations derived above, it is recommended to use (1) and (2), instead of (3) and (4); particularly if the system simulated in the real-time simulator has distribution lines with low X/R. For simulations with transmission lines with high X/R (≈10 or higher), the expressions given by (3) and (4) can be used [9].

III. Proposed Method

The proposed method to interface a GFMI to a PHIL setup is depicted in Fig. 3. In the hardware side of the setup, the main difference with respect to the one shown in Fig. 1 is that now an inductor is placed between the GFMI and the power amplifier to avoid the instability issues previously mentioned. The contactor controls the interconnection between the two devices, and it is triggered by a digital signal from the real time simulator. In the simulation side, the voltage measured at the terminals of the GFMI is replicated in the controlled voltage source V_i. Notice that the inductor and the total resistance of the hardware side are also replicated inside the simulation, this forms a digital twin inside the real time simulator.

Following the simulated inductor and resistor, a virtual load bank is connected. Under this scenario, the loads inside the simulation are supplied by a replica of the voltage of the GFMI. The last step at hardware level is to make the power amplifier to emulate a load that mirrors the simulated loads, that way the GFMI will deliver the same amount of real and reactive power as its simulated counterpart. One way to fulfill this constraint would be to measure the voltage at bus B1 inside the simulation and use it to drive the power amplifier. Thus, by (1) and (2), the real and reactive powers delivered by the GFMI to the power amplifier matches the real and reactive powers delivered by V_i to the simulated loads ($P_H = P_S$ and $Q_H = Q_S$).

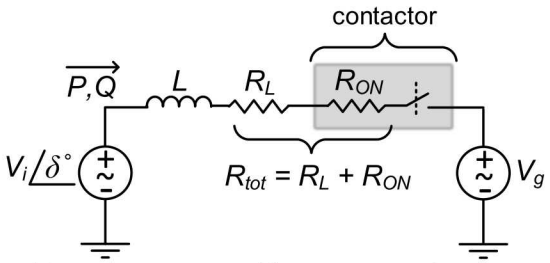

Fig. 2. Two voltage sources with a reactor as an interface between them.

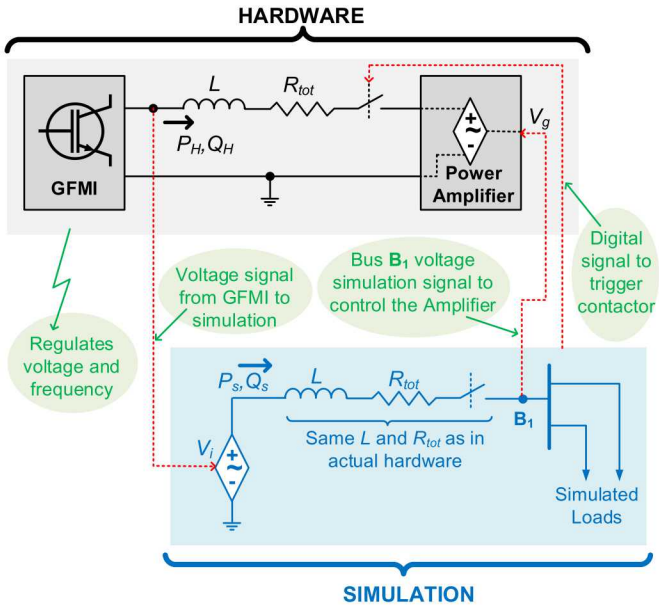

Fig. 3 Proposed method to interface GFMIs into PHIL setups.

This result holds only if an accurate measurement of the inductor value and the corresponding series resistance is obtained. The most important characteristic of this setup is that now the inverter itself is the element that regulates the voltage and frequency of the entire system.

In simulation, if a voltage source is present at bus B1, then both the GFMI and simulated voltage source must have load sharing capabilities in their control schemes, such as droop-control or VOC. The absence of load sharing capabilities on either side of the setup can lead to the unstable scenario previously described. Since some commercial GFMIs do not provide droop-control capabilities, the corresponding PHIL setup must not include voltage sources on the load side of the simulation. Their standalone (isochronous [9]) functionality can be tested by using simulated real and reactive loads, as it is the case described in the next section.

IV. Experimental Setup

In order to validate the proposed method, a commercially available GFMI was interfaced with a power amplifier in a PHIL simulation. Since the inverter does not provide droop-control capabilities, the PHIL tests were performed only in asynchronous mode, were the GFMI is the only source of power inside the system. The tests were conducted in the PHIL testbed located at Sandia National Laboratories' Distributed Energy Technologies Laboratory (DETL) [6]. A detailed diagram of the testing setup is depicted in Fig. 4. The GMFI under test is a single-phase unit rated for 5.0 kVA at 240 V in a split-phase configuration. At the DC bus, the GFMI is connected to a Valve-Regulated Lead-Acid (VRLA) battery, rated for 390 Ah at 48 V_{DC}. At the AC side, due to the split-phase configuration, two inductors of the same nominal value were used to sustain balanced conditions. Detailed measurements were taken for each inductor (L_1, L_2) and their corresponding series resistances (R_1, R_2), along for the resistances of each contactor (R_{ON1}, R_{ON2}). Table 1 summarizes those measurements. The neutral connection between the GFMI and the power amplifier is solidly grounded in the amplifier side.

Table 1. Inductor and resistor values.

L_1	1.29 mH @ 60 Hz	L_2	1.24 mH @ 60 Hz
R_1	0.0325 Ω	R_2	0.0475 Ω
R_{ON1}	0.11 Ω	R_{ON2}	0.095 Ω

The single-phase circuit was implemented in real-time HIL simulation, where the values of L_S and R_S include the total inductance and resistance around the two lines in the split-phase configuration of the hardware side, which gives:

$$L_S = L_1 + L_2 \tag{5}$$

$$R_S = R_1 + R_2 + R_{ON1} + R_{ON2} \tag{6}$$

Two 1.5 kW virtual loads were placed in the real-time simulation, while the voltage at bus B1 was used as the analog input of the power amplifier. Since the X/R of this particular case is low (< 10), the resistance given by (6) cannot be ignored.

To start the PHIL simulation, the following steps were followed:

1. Take an accurate measurement of the external inductor value and its resistance. Also, measure the resistance of the contactor. Make sure those values are replicated in the simulation.

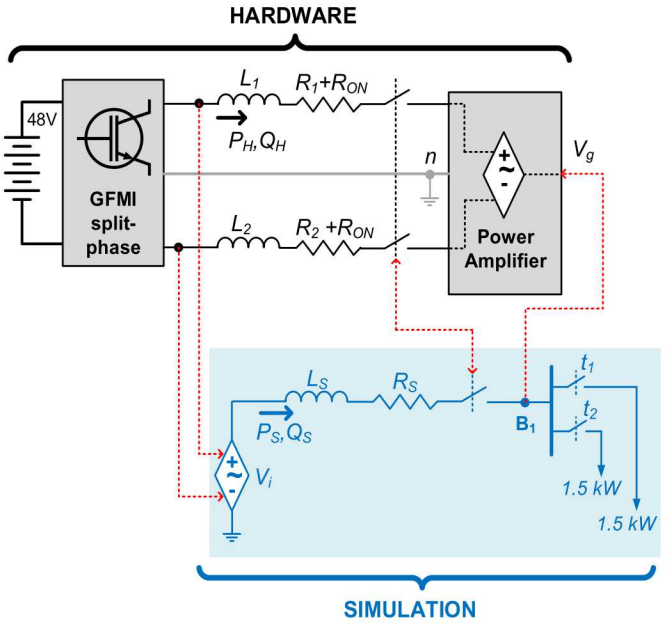

Fig. 4 PHIL experimental setup using a power amplifier with real-time simulation to emulate different load levels on a GFMI.

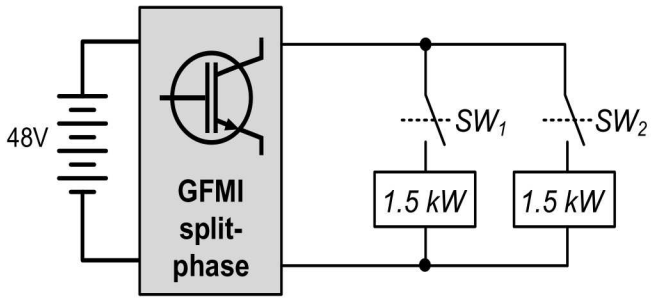

Fig. 5. Experimental setup of GFMI connected to a resistive load bank.

2. With the contactor open, turn on the GFMI under test and configure its settings to grid-forming mode. Start the simulation. At this point, an open circuit voltage should be measured at the terminals of the inverter and that reading is passed to the simulation.
3. In the simulation, turn on the simulated contactor and let the simulation reach its steady state. At this point, the Hardware-in-the-Loop has not been completed since there is no energy being transferred from the GFMI to the power amplifier.
4. Activate the contactor with the digital signal from the simulator box.
5. Check for stability and compare the real and reactive powers: $P_H \approx P_S$, and $Q_H \approx Q_S$.
6. If the real and reactive powers of the GMFI are not close to their counterpart in the simulation, then the values of L_S and R_S can be modified accordingly until the errors are reduced.

V. Experimental Setup

In order to verify the stability and accuracy of the proposed method, the two simulated loads of 1.5 kW, shown in Fig. *4*, were configured to switch in a staircase sequence (upwards and downwards) and compared to the results from the same test with a physical load bank shown in Fig. 5. This way, the step changes in real power expose the dynamics and stability of the transient behavior of the GMFI, as well as the corresponding accuracy of the steady state values.

Plots of the real and reactive powers from the PHIL simulation and the load bank are shown in Fig. 6. The overlap in the curves shows that the method not only is stable under abrupt load changes, but also that the accuracy between the three measurements is within 5 percent of error. The power factor was maintained close to unity due to the resistive nature of the loads. A slight amount of reactive powers is present due to the reactance of output LC filter inside the GFMI [6].

Fig. 7 shows the traces of current, voltage, and frequency of the GFMI, respectively. These traces corroborate the grid-forming nature of the inverter as the voltage and frequency are regulated as the currents step up or down, following load demands. The voltage is regulated around 243 V_{rms}, with very little distortion during load transitions. Additionally, the frequency shows no visible distortion around its nominal value of 60 Hz.

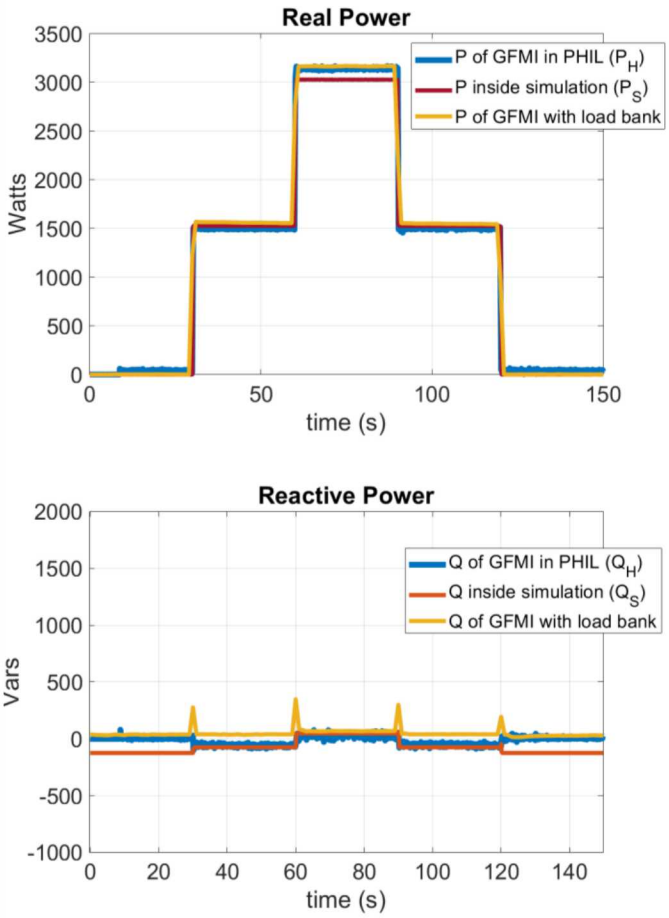

Fig. 6. Real and reactive power dynamics using the PHIL setup and the load bank.

I. Conclusions

A method and a procedure to interface GFMIs into a PHIL setup are proposed. In order to avoid the conflict of connecting the GFMI directly to the terminals of a power amplifier, an inductor is placed between the two devices. This permits the flow of energy while the GFMI regulates the voltage and frequency of the entire PHIL system. The results demonstrate the ability of the power amplifier and real-time HIL simulation to act as a controllable load. This method was validated against data obtained by testing the GFMI under real loads. Experimental data showed that the method is stable under step changes in the load requirements. The accuracy of the method is strongly related to the accuracy of the measurements of the external inductor value, and its corresponding series resistance.

As GFMI control methods are constantly evolving, this method provides the foundations of incorporating such devices into PHIL simulations, which eventually can help to develop automated testing procedures to verify GFMI functionality for standards compliance. This method can also be used to replace the use of discrete load banks, where sometimes the exact load cannot be achieved by the combination of discrete loads. With the proper selection of the external inductor, the power amplifier can play the role of a programmable and continuous load. PHIL simulations also allow creation of digital twins of power systems to test GFMIs under a wide variety of operational scenarios and applications.

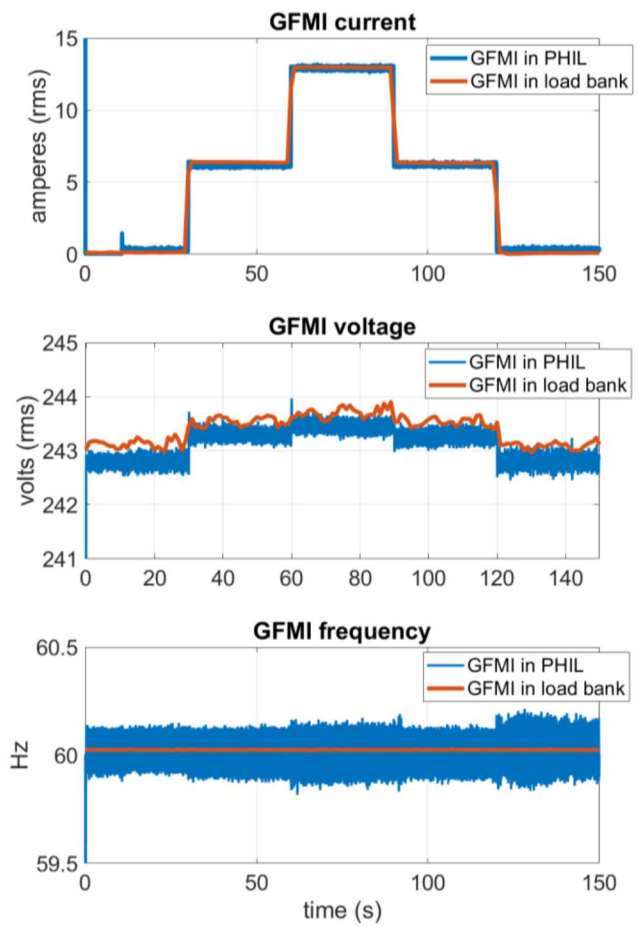

Fig. 7. Current, voltage, and frequency dynamics using the PHIL setup and the load bank.

ACKNOWLEDGMENT

Sandia National Laboratories is a multi-mission laboratory managed and operated by National Technology and Engineering Solutions of Sandia, LLC. a wholly owned subsidiary of Honeywell International, Inc., for the U.S Department of Energy's National Nuclear Security Administration under contract DE-NA-0003525.

REFERENCES

[1] N. Abi-Samra, *Power Grid Resiliency for Adverse Conditions*. San Diego: Artech House, 2017.

[2] B. J. Walker, "Developing a Resilience Model for North America's Energy Sector Infrastructure," Washington, DC, 2019.

[3] R. H. Lasseter and P. Piagi, "Microgrid: A Conceptual Solution," in *PESC*, 2004.

[4] DOE, "The Role of Microgrids in Helping to Advance the Nation's Energy System | Department of Energy," 2015. [Online]. Available: https://www.energy.gov/oe/activities/technology-development/grid-modernization-and-smart-grid/role-microgrids-helping. [Accessed: 02-Nov-2019].

[5] J. Johnson, R. Ablinger, R. Bruendlinger, B. Fox, and J. Flicker, "Interconnection Standard Grid-Support Function Evaluations Using an Automated Hardware-in-the-Loop Testbed," *IEEE J. Photovoltaics*, vol. 8, no. 2, pp. 565–571, Mar. 2018.

[6] J. Hernandez-Alvidrez and J. Johnson, "Parametric PV Grid-Support Function Characterization for Simulation Environments," in *2017 IEEE 44th Photovoltaic Specialist Conference (PVSC)*, 2017, pp. 2153–2158.

[7] R. Teodorescu, M. Liserre, and P. Rodríguez, *Grid Converters for Photovoltaic and Wind Power Systems*, First. Wiley, 2011.

[8] B. Kroposki *et al.*, "Achieving a 100% Renewable Grid: Operating Electric Power Systems with Extremely High Levels of Variable Renewable Energy," *IEEE Power Energy Mag.*, vol. 15, no. 2, pp. 61–73, 2017.

[9] P. Kundur, *Power System Stability and Control*. Tata McGraw-Hill, 1993.

[10] W. Du, K. P. Schneider, F. K. Tuffner, Z. Chen, and R. H. Lasseter, "Modeling of Grid-Forming Inverters for Transient Stability Simulations of an all Inverter-based Distribution System," pp. 1–5, 2019.

[11] H. Bevrani, B. François, and T. Ise, *Microgrid Dynamics and Control*. New Jersey: Wiley & Sons, 2017.

[12] H. K. Khalil, *Nonlinear systems*. PEARSON, 2014.

[13] B. B. Johnson, M. Sinha, N. G. Ainsworth, F. Dorfler, and S. V. Dhople, "Synthesizing Virtual Oscillators to Control Islanded Inverters," *IEEE Trans. Power Electron.*, vol. 31, no. 8, pp. 6002–6015, Aug. 2016.

[14] J. Brian, L. Yashen, E. Joe, L. Robert, E. Abraham, and D. Kirshen, "Grid-forming Inverters for Low-inertia Power Systems," *Workshop on Low-inertia Grids. Univertsity of Washington.*, 2019. [Online]. Available: https://lowinertiagrids.ece.uw.edu/. [Accessed: 02-Nov-2019].

[15] *IEEE Std 1547-2018 (Revision of IEEE Std 1547-2003) : IEEE Standard for Interconnection and Interoperability of Distributed Energy Resources with Associated Electric Power Systems Interfaces.* IEEE, 2018.

[16] UL-1741, "Standard for Inverters, Converters, Controllers and Interconnection System Equipment for Use With Distributed Energy Resources," 2010.

[17] International Electrotechnical Commission, "IEC 61850-90-7," 2013.

[18] RTDS Technologies, "Power Hardware in the Loop Simulations (PHIL report)," 2018.

[19] S. Chakraborty, A. Nelson, and A. Hoke, "Power hardware-in-the-loop testing of multiple photovoltaic inverters' volt-var control with real-time grid model," in *2016 IEEE Power & Energy Society Innovative Smart Grid Technologies Conference (ISGT)*, 2016, pp. 1–5.

[20] M. Panwar, S. Suryanarayanan, and S. Chakraborty, "Steady-state modeling and simulation of a distribution feeder with distributed energy resources in a real-time digital simulation environment," in *2014 North American Power Symposium (NAPS)*, 2014, pp. 1–6.

[21] W. Ren, M. Steurer, and T. L. Baldwin, "Improve the Stability and the Accuracy of Power Hardware-in-the-Loop Simulation by Selecting Appropriate Interface Algorithms," *IEEE Trans. Ind. Appl.*, vol. 44, no. 4, pp. 1286–1294, 2008.

[22] J. Hernandez-Alvidrez, A. Summers, M. J. Reno, J. Flicker, and N. Pragallapati, "Simulation of Grid-Forming Inverters Dynamic Models using a Power Hardware in the Loop Testbed.," in *46th IEEE Photovoltaic Specialists Conference*, 2019, no. July.

[23] J. Hernandez-Alvidrez *et al.*, "PV-Inverter Dynamic Model Validation and Comparison Under Fault Scenarios Using a Power Hardware-in-the-Loop Testbed," in *2018 IEEE 7th World Conference on Photovoltaic Energy Conversion (WCPEC) (A Joint Conference of 45th IEEE PVSC, 28th PVSEC & 34th EU PVSEC)*, 2018, pp. 1412–1417.